JAERI-Research
98-031

ESTIMATION OF LONGITUDINAL AND TRANSVERSE DISPERSIVITIES IN THE TWIN LAKE NATURAL GRADIENT TRACER TESTS

June 1998

Seiji TAKEDA and Greg L. MOLTYANER*

日本原子力研究所
Japan Atomic Energy Research Institute

本レポートは，日本原子力研究所が不定期に公刊している研究報告書です。
入手の問合わせは，日本原子力研究所研究情報部研究情報課（〒319-1195　茨城県那珂郡東海村）あて，お申し越しください。なお，このほかに財団法人原子力弘済会資料センター（〒319-1195　茨城県那珂郡東海村日本原子力研究所内）で複写による実費頒布をおこなっております。

This report is issued irregularly.
Inquiries about availability of the reports should be addressed to Research Information Division, Department of Intellectual Resources, Japan Atomic Energy Research Institute, Tokai-mura, Naka-gun, Ibaraki-ken, 319-1195, Japan.

編集兼発行　　日本原子力研究所

JAERI-Research 98-031

Estimation of Longitudinal and Transverse Dispersivities in the Twin Lake Natural Gradient Tracer Tests

Seiji TAKEDA and Greg L. MOLTYANER*

Department of Environmental Safety Research
Nuclear Safety Research Center
Tokai Research Establishment
Japan Atomic Energy Research Institute
Tokai-mura, Naka-gun, Ibaraki-ken

(Received May 13, 1998)

The field scale tracer tests were carried out with a non-reactive tracer of ^{131}I at Twin Lake on the Chalk River Laboratory (CRL) site in Atomic Energy of Canada Limited (AECL). The natural gradient dispersion test such as the Twin Lake tracer test is very few and useful for evaluating mass transport parameters and testing groundwater flow and transport models.

In this report, mass transport parameters, velocity, longitudinal and transverse dispersivities, were estimated from the Twin Lake 40 m tracer tests. This estimation was performed to provide dispersion data for 3-D transport modelling in the Lake 233 site scale (600 m in east-west direction and 1400 m in north-south direction). Two different methods were applied to the measured breakthrough curves of ^{131}I in order to evaluate velocity and longitudinal dispersivity. The first method is the fitting procedure of the 1-D advection-dispersion solution, and the second one is the temporal moments analysis. The effect of applying these methods to field data on transport parameters was discussed in this study. The vertical profiles of ^{131}I were used in the estimation of transverse dispersivity by fitting the 3-D advection-dispersion solution. This report refereed to the effect of variable velocity on the estimated dispersivities. The correlation between magnitude of both dispersivities and the travel distance up to 40 m was also investigated.

Keywords: Longitudinal and Transverse Dispersivities, Transport Parameter, Radioactive Waste Disposal, Least Square Fitting Method, Temporal Moments Analysis, Twin Lake Tracer Test

* Atomic Energy of Canada Limited (AECL)

自然条件下のTwin Lakeトレーサーテストにおける縦方向及び横方向分散長の評価

日本原子力研究所東海研究所安全性試験研究センター環境安全研究部
武田　聖司・Greg L. MOLTYANER*

(1998年5月13日受理)

カナダ原子力公社（ＡＥＣＬ）チョークリバー研究所のTwin Lakeサイトにおいて、^{131}Iを用いたフィールド規模のトレーサー試験が実施された。Twin Lakeトレーサー試験のような自然水理条件下での実験は少なく、移行パラメータの評価や地下水及び核種移行モデル検証に有効である。移行パラメータである流速、縦方向及び横方向分散長を40m規模のTwin Lakeトレーサー試験から評価した。これは、Lake 233サイト規模（東西 600m、南北1400m）の3次元移行モデルに必要な移行パラメータを推定するためである。流速、縦方向分散長の算定のために、実測された破過曲線に対し2種類の方法を適用した。1つは1次元移流－分散方程式の解であり、もう1つは統計的手法である時間的モーメントの適用である。推定された移行パラメータに対するこれらの方法の適用性について議論した。また、横方向分散長は3次元移流－分散方程式の解を^{131}Iの鉛直方向の濃度分布に適用することにより求めた。試験エリア内では透水性の異なる地層が確認され、透水性の違いが分散長に及ぼす影響について報告した。また、推定された縦方向及び横方向分散長と40mまでの移行距離との相関についても議論した。

東海研究所：〒319－1195　茨城県那珂郡東海村白方白根2－4
＊ カナダ原子力公社

Contents

目　　次

This is a blank page.

1. Introduction

The field scale dispersion tests were carried out with a gamma-emitting radioactive tracer (^{131}I) at the Twin Lake tracer test site in 1982 and 1983. The objectives of the Twin Lake tracer experiments are to research geologic heterogeneity, hydraulic and dispersive properties and to provide data for developing and evaluating groundwater flow and transport models. There are very few field values of mass transport parameters such as longitudinal and transverse dispersivities determined from natural gradient dispersion tests. Therefore, the transport parameters determined from the Twin Lake natural gradient experiment are valuable and useful for testing flow and transport models.

The breakthrough curves of ^{131}I measured at each monitoring point were used in the estimation of longitudinal dispersivity and velocity with two methods. In the first method, an observed breakthrough curve was fitted to one simulated using the solution of the one-dimensional advective-dispersive equation, which have been reported by Moltyaner and Paniconi (1984)[1] and Moltyaner and Killey (1988a)[2]. The best estimated value in fitting procedure is achieved using the least squares method. The second method is based on the temporal moments analysis and has been applied to the characterization of mass transport by Devary and Simmons (1984)[3] and Moltyaner and Wills (1987)[4]. In this work, the transport parameters estimated by both the fitting and temporal moment methods were compared and the effect of applyi -ng two methods to the measured breakthrough curves on the estimation of transport parameters was discussed. The vertical profiles of ^{131}I collected at each borehole along the tracer path were used in the estimation of transverse dispersivity by fitting the three-dimensional advection-dispersion solution to an observed vertical profile. In this simulation, the estimated values of velocity and longitudinal dispersivity were treated as the fixed input parameters. The hydraulic heterogeneity was characterized as variability in the velocity zone within the tracer flow area at the Twin Lake site, and the distribution of velocity was discussed by Killey and Moltyaner (1988)[5]. The effect of variable velocity on both longitudinal and transverse dispersivities was discussed in this work. Magnitude of aquifer dispersivities is often considered to increase with the increase of measurement scale. Therefore, the relation between magnitude of each dispersivity and the measurement scale until the travel distance of 40 m was also investigated in this study.

2. Twin Lake Tracer Tests

Figure 1 shows the location of the Twin Lake natural gradient tracer tests, which were performed using non-reactive radiotracer (^{131}I) over 20 and 40 m distances in 1982 and 1983. This research site is located at the northwest of Twin Lake and between Pitcher Plant Swamp and Twin Lake. This swamp is the discharge area of groundwater flow in this site. The groundwater flow in this study area is predominantly in the horizontal direction from east of

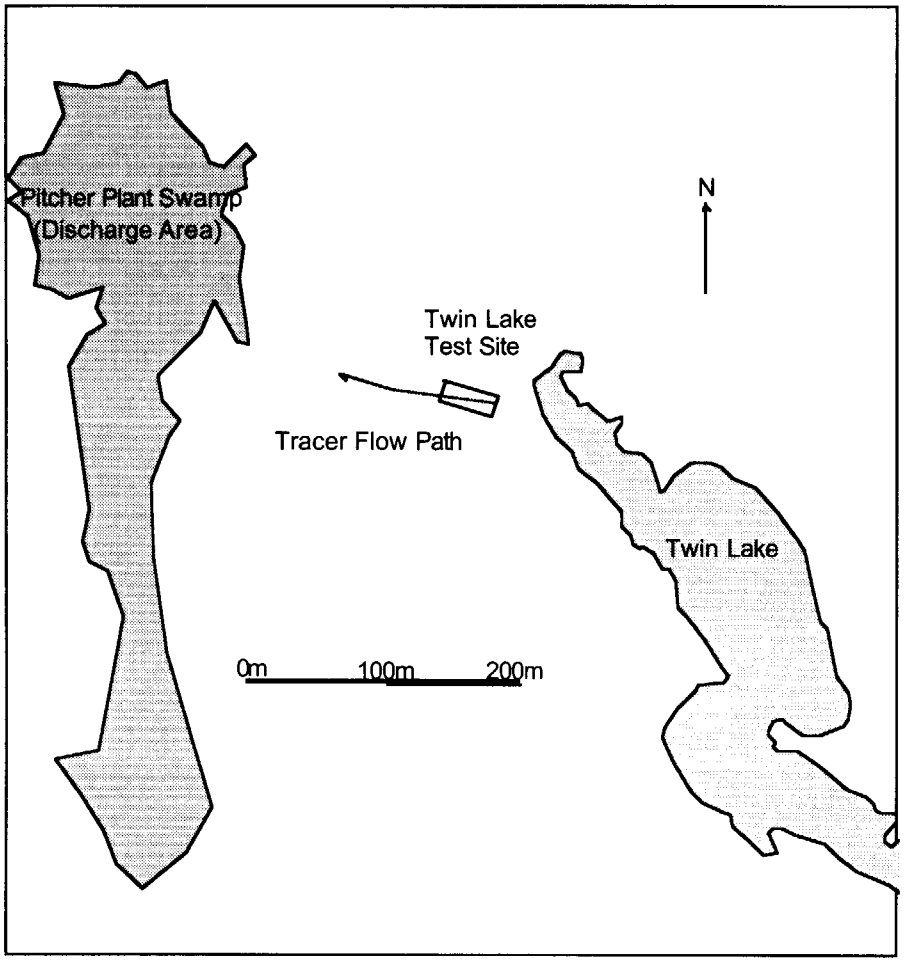

Figure 1 Location of Twin Lake Tracer Test Site

Twin Lake to northwest, toward a groundwater discharge area. Twin Lake has one seasonal surface inlet and no surface outlets. The lake drains by recharging the underlying sands.

For the evaluation of the Twin Lake tracer test site, many hydrogeologic data such as stratigraphic information, hydraulic head, hydraulic conductivity and porosity have been collected at all boreholes location. From the measurements of hydraulic head, most of the aquifer recharge occurs during the spring melt, with an occasional minor recharge in November-December. Although aquifer hydraulic heads vary by up to 1.5 m annually, the fluctuation of hydraulic head are similar in magnitude and timing throughout the Twin Lake tracer test area. Flow directions and velocities in this test site are considered to remain relatively constant.

Figure 2 shows the location of monitoring points with the local coordinate at the 40 m tracer test site. A set of boreholes was drilled at every five meter to east-west direction, which corresponded with main direction of groundwater flow at the tracer test site. The center of tracer flowpath is also given in Figure 2. The cross section along this flowpath is also shown in Figure 3. The borehole number is represented by 2W0S, 5W0.5S, 10W1.5S and so on. For instance, 10W1.5S means the location of 10 m west and 1.5 m south from the injection well. The migration

of non-reactive tracer ^{131}I was monitored in the array of these boreholes penetrating the full thickness of the Twin Lake aquifer. The general geology of Twin Lake aquifer is typified by fine-medium sands unit overlying the bedrock. The elevation of the upper limit of tracer flowpath ranges from 145 to 149 m over the bedrock surface. The thickness of the saturated sands from the injection well to 40W7S borehole is approximately from 9 to 10 m. Based on the estimation of hydraulic conductivity within the tracer flow zone, the fine-medium sands unit was classified into three velocity regions [Killey and Moltyaner (1988)[5]]. Figure 3 also shows the distribution of hydraulic conductivity along the center of the tracer flowpath. Region A, D and E correspond to the high velocity region, region B to the intermediate velocity region and region C and F to the low velocity region. There is a layered inhomogenity in velocity in the fine-medium sands unit at the Twin Lake site. The estimation of mass transport parameters was carried out for these velocity regions.

The non-reactive tracer of ^{131}I was spiked with constant flow rate and injected into the Twin Lake aquifer at uniform concentration for 8.2 hours. Total injection volume was 5.78 m3. During the field-scale tracer tests, two types of measurements were collected using dry access tubes. One is the continuous depth distribution of gamma activity at discrete points in time and used in the estimation of transverse dispersivity. Another is the continuous time records of gamma activity at discrete depths and used in the estimation of longitudinal dispersivity. The measurement of gamma activity of radioiodine at the monitoring points was performed using NaI or geiger detectors hung in the dry access tubes and continued for 45 days.

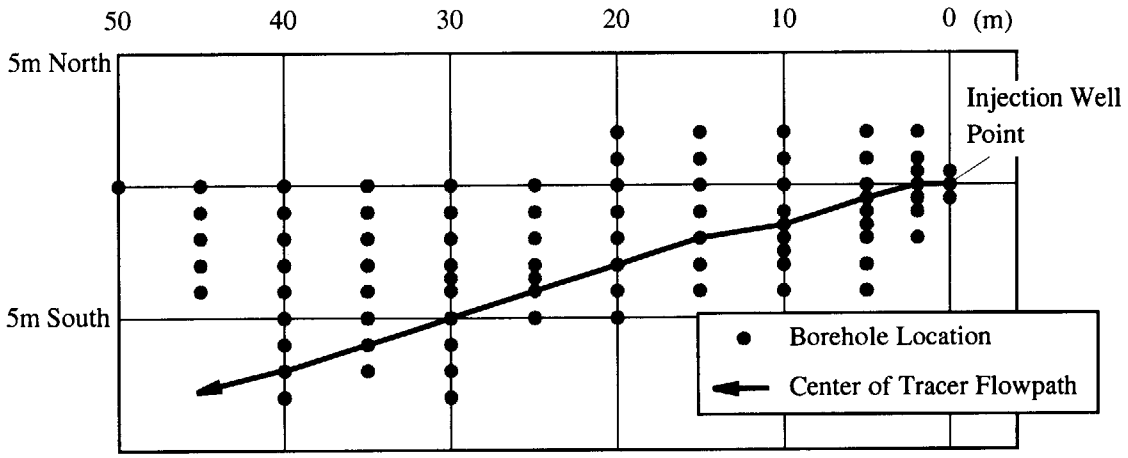

Figure 2 Location of injection well, monitoring points and tracer flowpath at Twin Lakesite

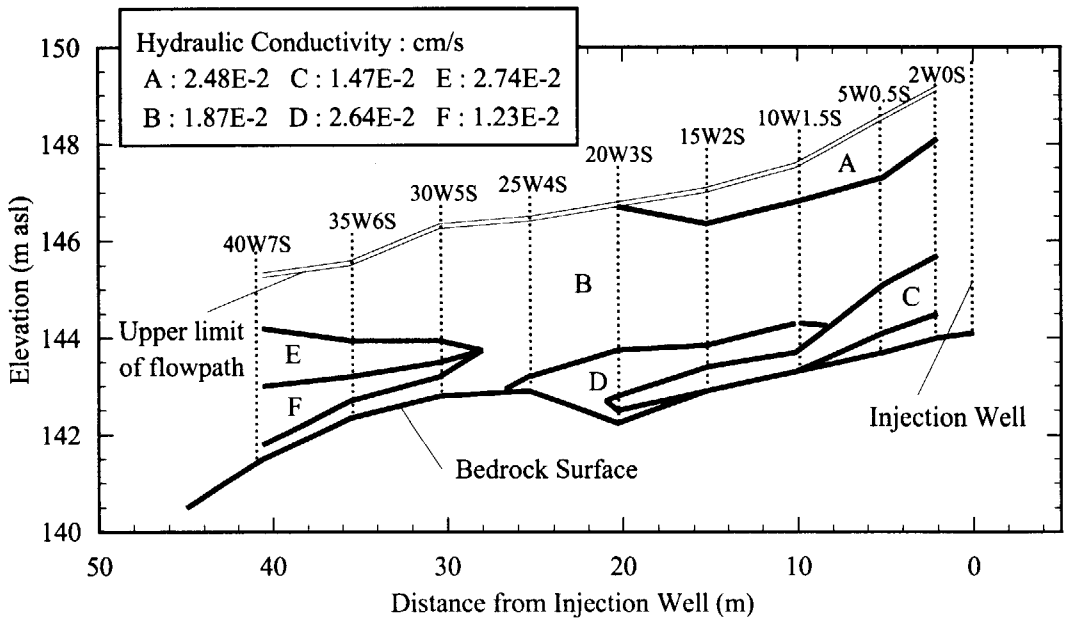

Figure 3 Hydraulic conductivity distribution along the tracer flow path [Killey and Moltyaner, 1988][5]

3. Mathematical Model

3.1 Least Squares Fitting

The advection-dispersion equation is generally accepted deterministic model that describes the transport of a conservative tracer in saturated porous media. Postulating steady state flow condition and choosing the x axis of the Cartesian coordinate system along the direction of the mean flow velocity V, the governing tracer transport equation with constant coefficients was written in the following form according to Bear, J. (1972)[6],

$$\frac{\partial C}{\partial t} = D_L \frac{\partial C}{\partial x^2} + D_{TL} \frac{\partial C}{\partial y^2} + D_{TV} \frac{\partial C}{\partial z^2} - V \frac{\partial C}{\partial x} \tag{1}$$

where t is time; C is the tracer concentration (ML^{-3}); D_L, D_{TL} and D_{TV} are the longitudinal (in the direction of flow), lateral-transverse (perpendicular to the direction of flow in xy plane) and vertical-transverse (perpendicular to the direction of flow in xz plane) hydrodynamic dispersion coefficients (M^2T^{-1}). In the case of homogeneous and isotropic media, the transverse dispersion coefficients are equal, $D_T = D_{TL} = D_{TV}$. The dispersivity coefficient are defined as the sum of

the coefficients of mechanical dispersion and molecular diffusion $D*$,

$$D_i = \alpha_i V + D^* \quad (i = L,TL,TV) \tag{2}$$

where α_i $(i = L,TL,TV)$ are the longitudinal and transverse components of dispersivity (M). In isotropic media, the transverse components are identical, $\alpha_{TL} = \alpha_{TV} = \alpha_T$. In the case that the effect of longitudinal dispersion is more predominant than that of transverse dispersion, the concentration gradients in the transverse direction can be ignored, and equation (1) is re-written as the one-dimensional form as follows,

$$\frac{\partial C}{\partial t} = D_L \frac{\partial C}{\partial x^2} - V \frac{\partial C}{\partial x} \tag{3}$$

Two types of analytical solutions for equation (1) and (3) were used to determine longitudinal and transverse dispersivities at the Twin Lake Tracer tests. The aquifer in this field tracer test is supposed to be of infinite extent in any directions of the coordinate system. Constant step input of tracer is also assumed in mathematical model. The solution of equation (1) was shown by Moltyaner and Killey (1988b)[7] and it has the following form,

$$C(x,y,z,t) = \frac{C_0}{8}\left[erf\left(\frac{x + x_0/2 - Vt}{2\sqrt{D_L t}}\right) - erf\left(\frac{x - x_0/2 - Vt}{2\sqrt{D_L t}}\right)\right]$$

$$\bullet\left[erf\left(\frac{y + y_0/2}{2\sqrt{D_{TL} t}}\right) - erf\left(\frac{y - y_0/2}{2\sqrt{D_{TL} t}}\right)\right]\bullet\left[erf\left(\frac{z + z_0/2}{2\sqrt{D_{TV} t}}\right) - erf\left(\frac{z - z_0/2}{2\sqrt{D_{TV} t}}\right)\right] \tag{4}$$

where x_0, y_0 and z_0 are initial dimensions of step input. The one-dimensional version of solution for equation (3) can be written as follows,

$$C(x,t) = 0.5C_0\left[erf\left(\frac{x + x_0/2 - Vt}{2\sqrt{D_L t}}\right) - erf\left(\frac{x - x_0/2 - Vt}{2\sqrt{D_L t}}\right)\right] \tag{5}$$

In order to estimate the values of longitudinal and velocity, the one-dimensional solution (5) was also applied to a measured breakthrough curve with the fitting procedure. The value of

transverse dispersivity was obtained by fitting an observed vertical profile of ^{131}I concentration to one simulated using the solution (4). The least squares method was used in the fitting procedure to obtain the best fit parameter values.

3.2 Temporal Moments Analysis

Another method for the estimation of transport parameters is the statistical moments. The statistical moments method was originally applied to mass transport problem by Van der Lann (1958)[8]. Temporal moments method is especially used in the evaluation of breakthrough curves. The tracer concentration-time moments for the one-dimensional case are defined as

$$M_n(x) = \int_0^\infty t^n C(x,t)dt \quad (n=0,1,2) \tag{6}$$

where M_n is the n-th (n=0,1,2) moment of concentration $C(x,t)$. Characterization of mass transport with the method of temporal moments has been performed by Devary and Simmons (1984)[3], Moltyaner and Wills (1987)[4] and others. Total mass, m_{tot}, leaving the system can be calculated from the following relationship,

$$m_{tot} = Q\int_0^\infty C(x,t)dt = Q \cdot M_0 \tag{7}$$

where Q is the tracer flow rate. The normalized n-th moment can be defined as follows,

$$m_n(x) = M_n(x)/M_0 = \int_0^\infty t^n C(x,t)dt / M_0 \tag{8}$$

The normalized zeroth moment, therefore, is equal to one ($m_0 = 1$). The normalized first moment can be written as follows.

$$m_1 = \int_0^\infty t \cdot C(x,t)dt / \int_0^\infty C(x,t)dt \tag{9}$$

The first moment is a quantity with the dimension of time. It may be thought of as the mean travel time of the tracer. The solution of the one-dimensional equation (3) for pulse input under the boundary condition of $C(x,t)|_{x=\pm\infty} = 0$ is

$$C(x,t)=\frac{m_{tot}}{Q}\frac{x}{2\sqrt{\pi D_L t^3}}\exp\left[-\frac{(x-Vt)^2}{4D_L t}\right] \tag{10}$$

The time moments can be computed with the basis of solution (10), and the normalized first moment is calculated from relationship (7), (9) and (10) as follows,

$$m_1=\int_0^\infty \frac{m_{tot}}{Q}\frac{x}{2\sqrt{\pi D_L t}}\exp\left[-\frac{(x-Vt)^2}{4D_L t}\right]dt/M_0=\frac{x}{V}=t_m \tag{11}$$

where t_m is the mean travel time. The n-th temporal moments about the mean travel time can be defined as,

$$\mu_n(x)=\int_0^\infty (t-m_1)^n\cdot C(x,t)dt/M_0 \tag{12}$$

The second moment about the mean travel time is written as follows,

$$\mu_2(x)=\int_0^\infty (t-m_1)^2\cdot C(x,t)dt/M_0 \tag{13}$$

The normalized second moment can be estimated from relationship (8) and (10) as follows,

$$m_2=\int_0^\infty \frac{m_{tot}}{Q}\frac{x}{2}\sqrt{\frac{t}{\pi D_L}}\exp\left[-\frac{(x-Vt)^2}{4D_L t}\right]dt/M_0=\frac{x}{V^3}(2D_L+Vx) \tag{14}$$

The variance of the concentration distribution can be obtained as follows,

$$\mu_2(x)=m_2-m_1^2=m_2-\left(\frac{x}{V}\right)^2=\frac{2D_L x}{V^3} \tag{15}$$

The zeroth, first and second temporal moments for the measured breakthrough curve are computed, and the mean travel time, average velocity and longitudinal dispersion are calculated from the relationships mentioned above.

3.3 Determination of Mass Transport Parameters

The breakthrough curves of ^{131}I measured at each monitoring point were used in the estimation of longitudinal dispersivity and velocity with two methods. In the first method, an observed breakthrough curve was fitted to one simulated using the one-dimensional solution (5). The best estimated value in fitting procedure is achieved using the least squares method. Another method is the temporal moments analysis, and these parameters are estimated using relationship (11) and (15) in previous section. The justification for applying the one-dimensional equation in both methods follows from the conclusion reported by Moltyaner and Paniconi (1984)[1]. They concluded that the breakthrough curves calculated along the 40 m tracer path using the 3-D solution is virtually identical to that obtained using the 1-D solution over the duration of the field experiments due to very low value of the transverse dispersivity.

For evaluating the transverse dispersivity, the technique of the least squares method are applied in experimental vertical profiles of ^{131}I concentration. The value of transverse dispersivity were decided from automatically fitting the 3-D solution (4) to a measured vertical profile. The parameter values of average velocity and longitudinal dispersivity were fixed in the fitting procedure. These fixed parameters were provided from the analysis of the time-concentration data.

It is considered that the spreading of the tracer due to molecular diffusion is negligibly small comparable with that due to mechanical dispersion, therefore the term of molecular dispersion is removed in relationship (2). The mass transport parameters are calculated under the assumption that the low, intermediate and high velocity regions in the tracer tests site are homogeneous and isotropic. The initial dimensions of step input, x_0, y_0 and z_0, were determined from a variety of regression fits, and the average value was used in all subsequent analyses.

4. Estimation of Velocity and Longitudinal Dispersivity

The breakthrough curves used in theanalysis are obtained from the measurements at monitoring points along the center of tracer flowpath as shown in Figure 2 and 3. The estimation of mass transport parameters was carried out for 8 data in low- and 11 data in intermediate- and 7 data in high-velocity region. Figure 4 shows the comparison of the estimated parameters between temporal moments method and fitting procedure in three velocity regions. From Figure 4 (a), there is little difference on the estimated velocity between temporal moments and least squares fitting. In the intermediate- and high-velocity region, however, the velocity estimated from fitting method is slightly higher than that from the moment method. Figure 4 (b) shows the comparison of longitudinal dispersivity. The longitudinal dispersivity obtained from the temporal moments analysis tends to be over-estimated. All values of longitudinal dispersivity from temporal moments are higher than that from fitting procedure in the intermediate- and high-velocity region.

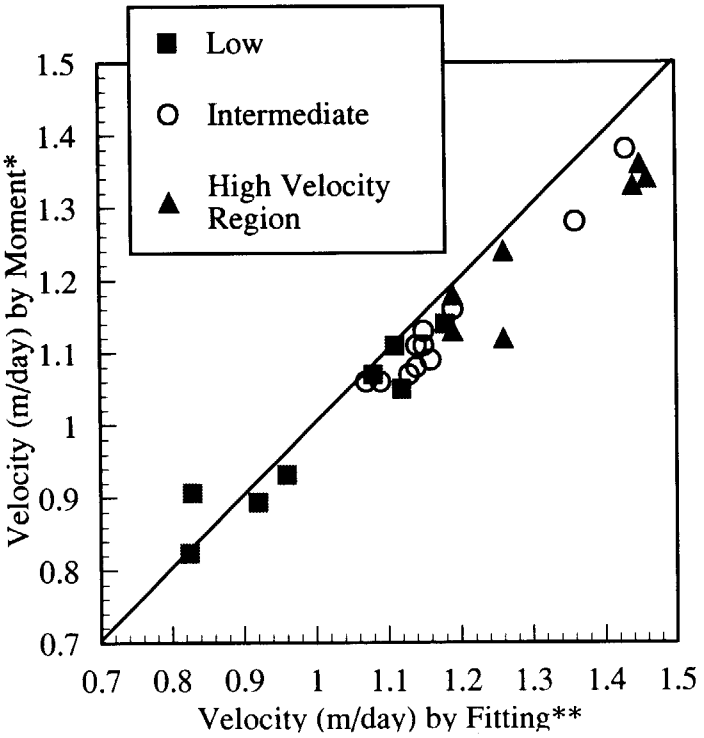

(a) Velocity

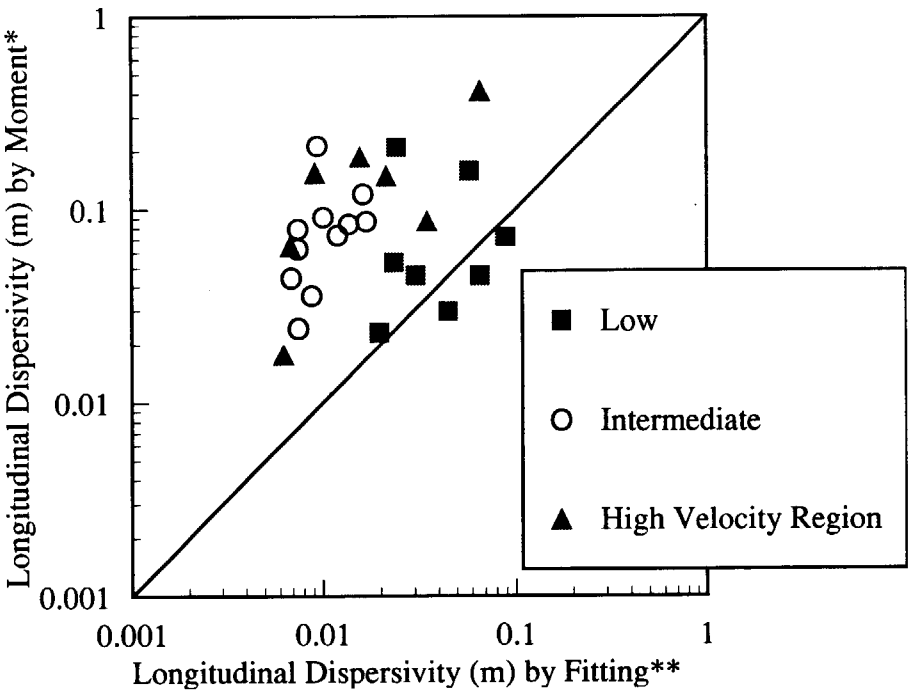

(b) Longitudinal Dispersivity

Figure 4 Comparison of the estimatedparameters between moment* (temporal moments method) and fitting** (1-D least squares method) in each velocity region

The relation between the estimated longitudinal dispersivity and the distance from injection well is shown in Figure 5. The average longitudinal dispersivity at the distance from the well is also plotted in Figure 5. Aquifer longitudinal dispersivity is often considered to increase with the increase of travel distance. This trend can be observed in the low velocity region. The value of longitudinal dispersivities estimated using two different methods are in good agreement except for the result at the distance of 35 m in the low velocity region. In the intermediate region of Figure 5 (b), the longitudinal dispersivities are hardly influenced by the increase of transport distance. The longitudinal dispersivity from the moments analysis are higher than that from the least squares fitting at all monitoring points. In Figure 5 (c), there is no effect of the travel distance on the longitudinal dispersion in the high velocity region. With respect to the comparison between two different methods, the same tendency is also recognized in the high velocity region.

Figure 6 shows the breakthrough curves of both measurements and simulations from the least squares fitting in the low velocity region. Equivalent comparison between measurement and simulation in the intermediate- and high-velocity region are also given in Figure 7 and 8, respectively. All measured breakthrough curves are classified into two types of data due to whether there is a effect of trailing tail in breakthrough curve or not. In the low velocity region, only the measured breakthrough curve at the borehole of 35W6S includes the trailing tail, and the estimated longitudinal dispersivities for this measurement are different between two methods as shown in Figure 5 (a). It is considered that discrepancy of longitudinal dispersivity between temporal moments and fitting method is caused by the effect of trailing tail because the effect of trailing tail is reflected on the temporal moment procedure but not on the fitting one. In the intermediate velocity region, the trailing tail can be obviously observed in all boreholes besides the borehole of 10W1.5S in Figure 7 (b). The discrepancy of dispersivity at the distance of 10 m is comparatively small as shown in Figure 5 (b). In Figure 5 (c) for the high velocity region, the dispersivities estimated from two methods at the distance of 5 and 20 m seem to be relatively close. The observed breakthrough curves at 5W0.5S and 20W3S in the high velocity region are given in Figure 8 (a) and (c), and do not include more effective part of trailing tail than the others. Thus it is suggested that the longitudinal dispersivity calculated using both time moments and least squares fitting methods depends on the trailing tail in measured breakthrough curve.

Figure 9 shows the variance of the estimated mass transport parameters in each velocity region. The mean values of velocity and longitudinal dispersivity are calculated from all estimated values and listed in Table 1. The result of the estimated velocity agrees with the classification of velocity zone determined by Killey and Moltyaner (1988)[5]. The mean velocities in the high-, intermediate- and low-velocity region are 1.28, 1.16, 0.997 m/day, respectively. The change of longitudinal dispersivity in the low velocity region relatively smaller than those in the intermediate and high velocity region. The larger variance of longitudinal dispersivity in the intermediate and high velocity region is caused by the different characteristic for evaluating mass transport parameters between temporal moments and least square fitting methods. However, there is little

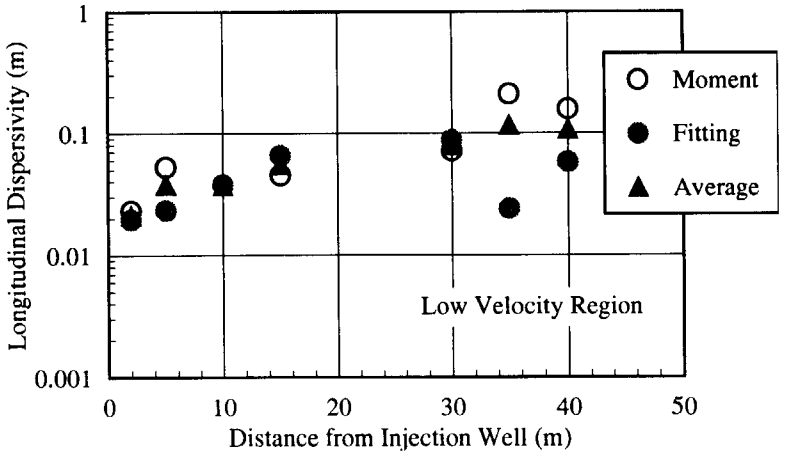

(a) Low Velocity Region

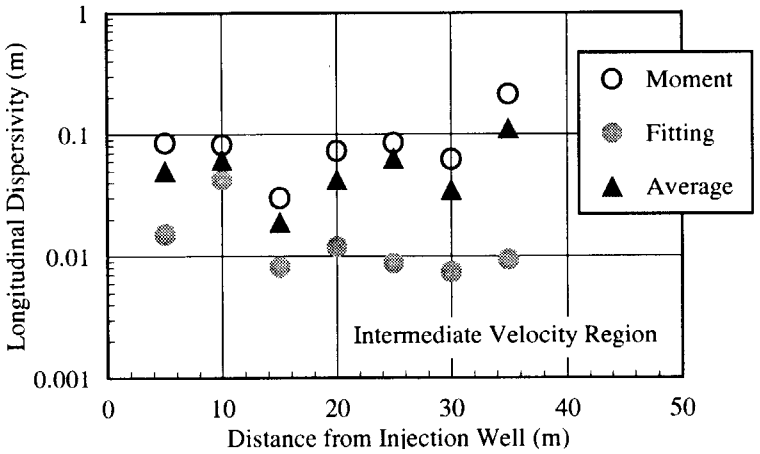

(b) Intermediate Velocity Region

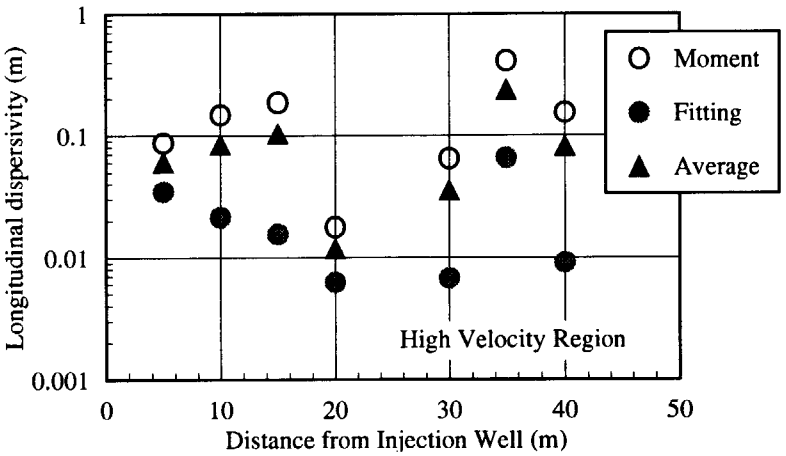

(c) High Velocity Region

Figure 5 Effect of the distance from injection well on the estimated longitudinal dispersivities in each velocity region

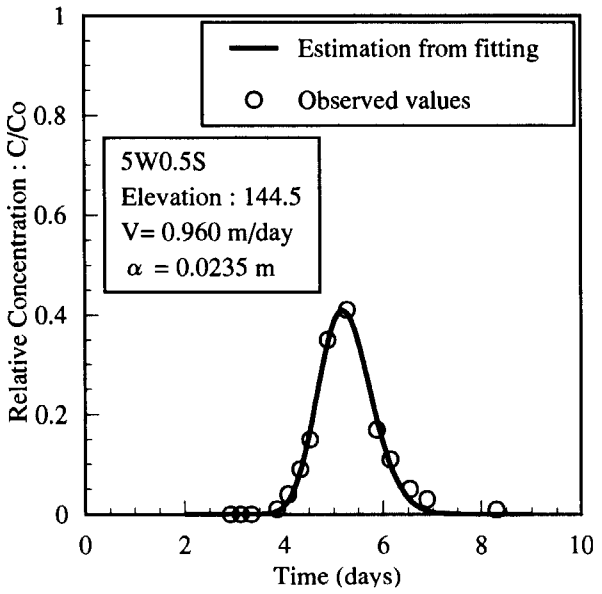

(a) 5W0.5S (elevation : 144.5m)

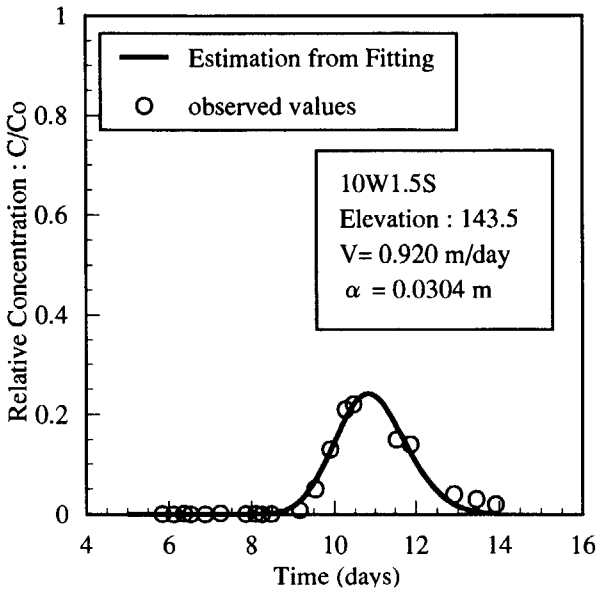

(b) 10W1.5S (elevation : 143.5m)

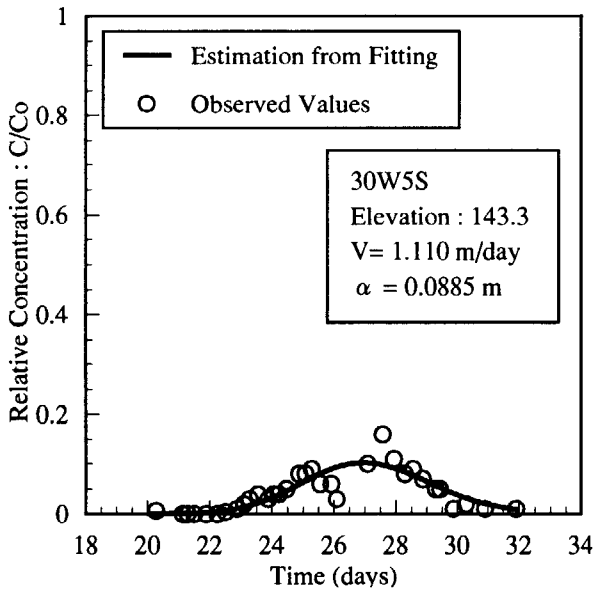

(c) 30W5S (elevation : 143.3m)

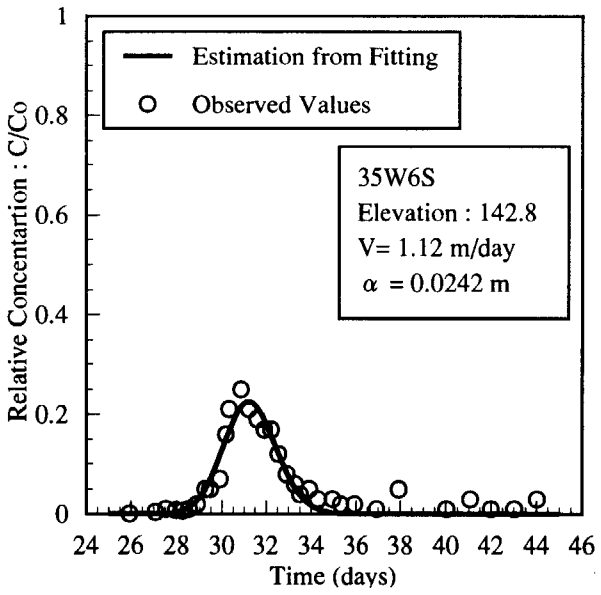

(d) 35W6S (elevation : 142.8m)

Figure 6 Breakthrough curves of measurement and simulation from the one-dimensional solution (5) in the low velocity region

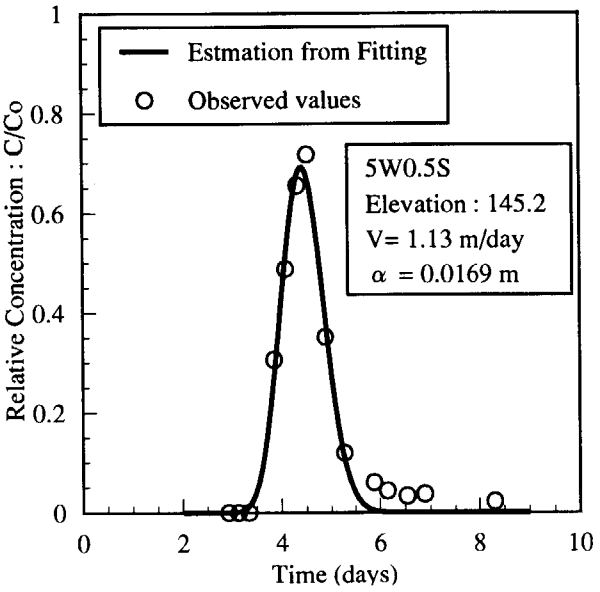

(a) 5W0.5S (elevation : 145.2m)

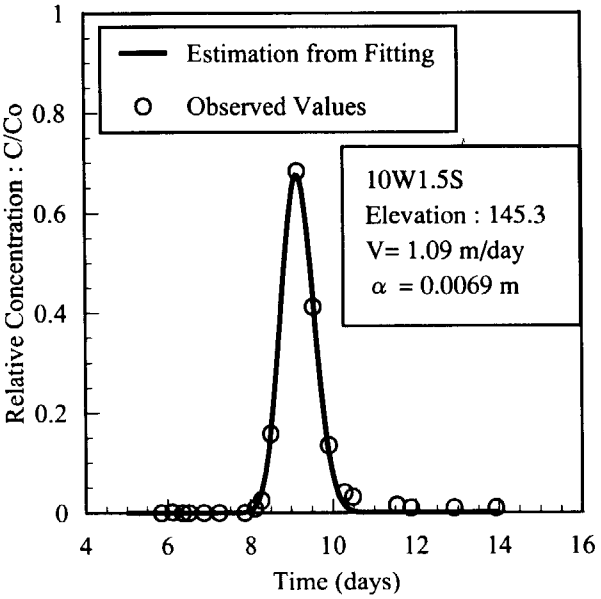

(b) 10W1.5S (elevation : 145.3m)

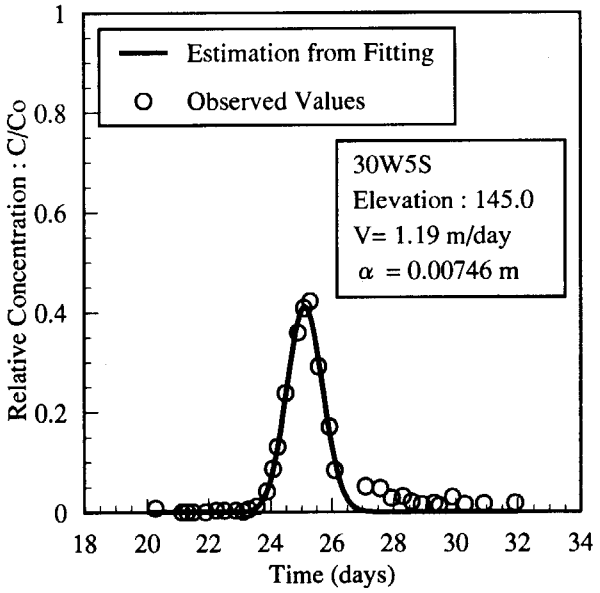

(c) 30W5S (elevation : 145.0m)

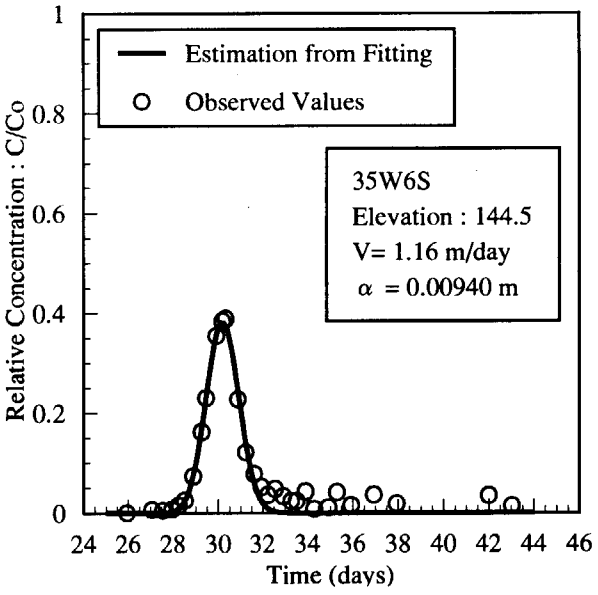

(d) 35W6S (elevation : 144.5m)

Figure 7 Breakthrough curves of measurement and simulation from the one-dimensional solution (5) in the intermediate velocity region

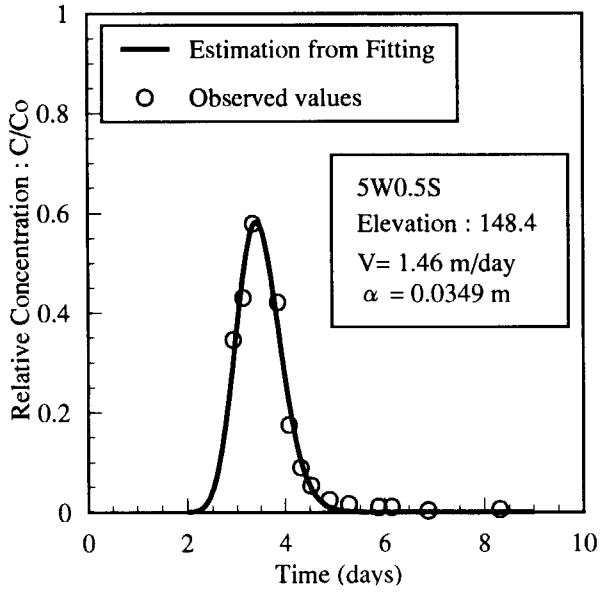

(a) 5W0.5S (elevation : 148.4m)

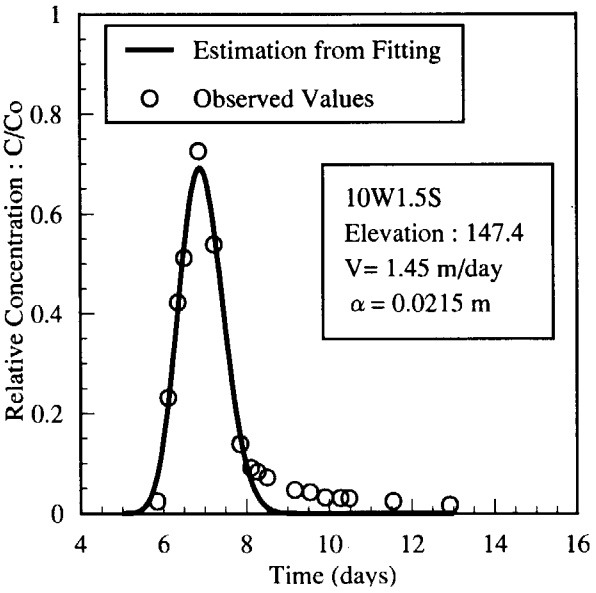

(b) 10W1.5S (elevation : 147.4m)

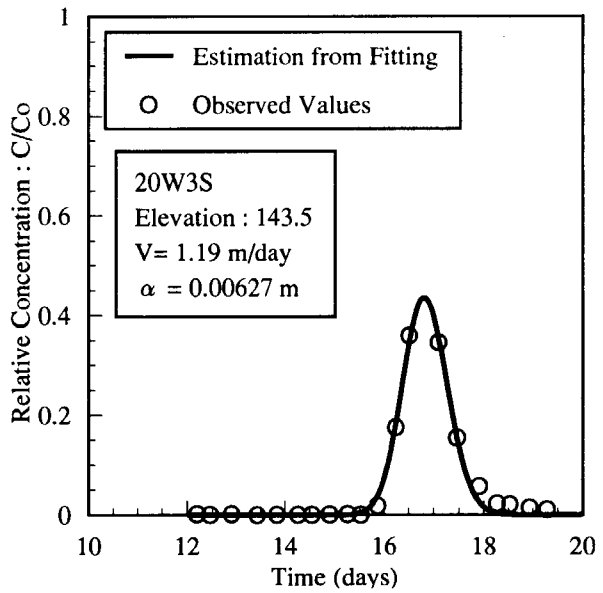

(c) 20W3S (elevation : 143.5m)

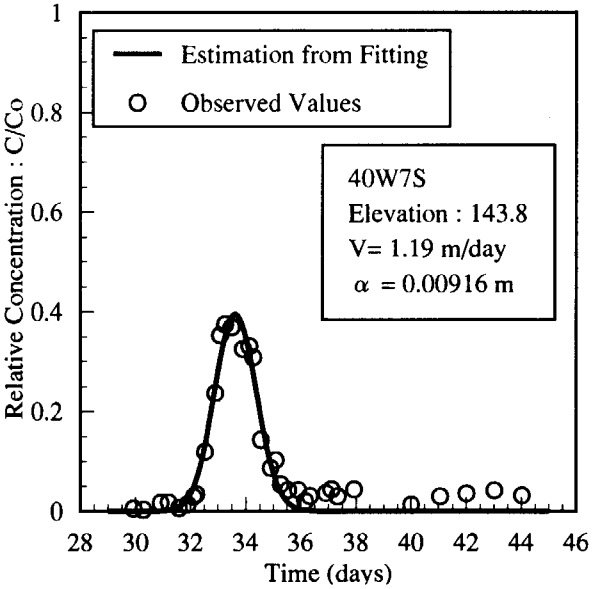

(d) 40W7S (elevation : 143.8m)

Figure 8 Breakthrough curves of measurement and simulation from the one-dimensional solution (5) in the high velocity region

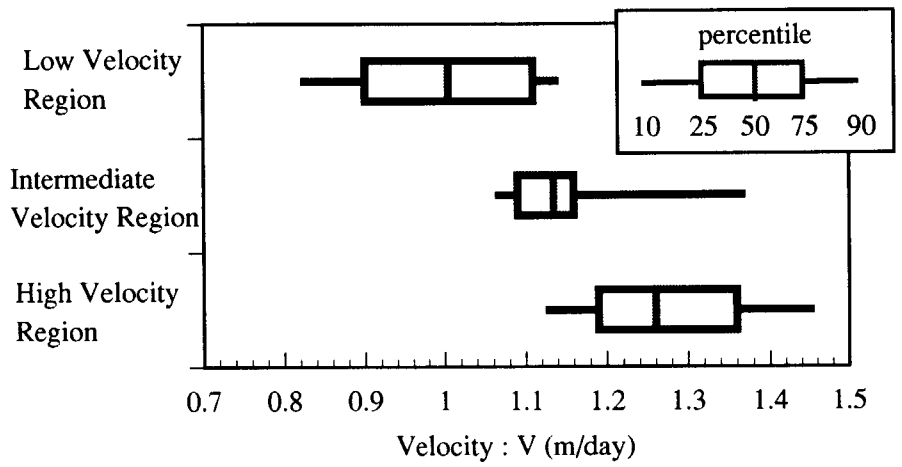

(a) Velocity

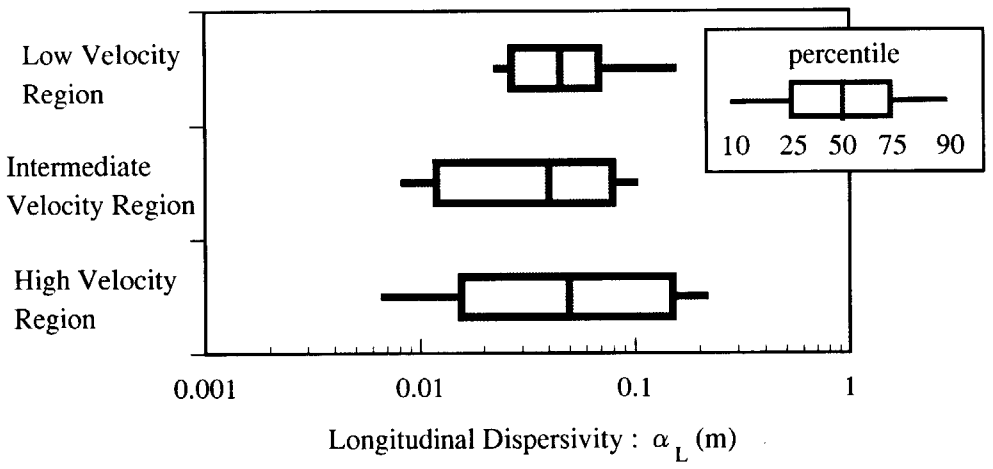

(b) Longitudinal Dispersivity

Figure 9 Variance of the estimated velocity and longitudinal dipersivity in the low, intermediate and high velocity region

Table 1 Average values of the estimated velocity and longitudinal dispersivity

Estimeted Parameters	High Velocity Region	Intermediate Velocity Region	Low Velocity Region
Mean Velocity : m/day	1.28	1.16	0.997
Mean Longitudinal Dispersivity : m	8.81×10^{-2}	5.27×10^{-2}	6.20×10^{-2}

difference of mean longitudinal dispersivity among the velocity regions as shown in Table 1.

5. Estimation of Transverse Dispersivity

The vertical profiles of ^{131}I at each borehole along the tracer path were used in the estimation of transverse dispersivity. The velocities and longitudinal dispersivities estimated in previous section were treated as the fixed input parameters in fitting the three-dimensional solution (4) to an observed vertical profile. Table 2 shows the result of transverse dispersivity in the low velocity region. The three-dimensional fitting technique was applied in Case A and Case B. In Case A, the fixed transport parameters were determined from the temporal moment analysis, and in Case B from the one-dimensional least squares fitting. To compare between measurement and simulation, the percent root mean squared error (RMSE) is calculated by the following formula given by Loague and Green (1991)[9],

$$RMSE(\%) = \left[\sum_{i=1}^{n}(P_i - O_i)^2 / n\right]^{1/2} / O_m * 100\% \qquad (16)$$

where n is the number of measurements, P_i and O_i are a predicted and an observed value, respectively and O_m is the average observed value. The values of RMSE for each result are also shown in Table 2. The value of RMSE at 15W2S is calculated to be higher than the others.

Table 2 The result of transverse dispersivity calculated from fitting the three-dimensional solution (4) to measuements in the low velocity region; in Case A using the fixed parameters of velocity and longitudinal dispersivity estimated from temporal moments, in Case B using ones estimated from least squares fitting

Well No. (Time:days)	Case	Velocity : V(m/day)	Longitudinal Dispersivity : α_L(m)	Tnansverse Dispersivity : α_T(m)	RMSE (%)
5W0.5S (6.15)	A	0.932	5.31×10^{-2}	8.09×10^{-4}	18.3
	B	0.960	2.35×10^{-2}	2.58×10^{-4}	19.8
5W0.5S (6.54)	A	0.932	5.31×10^{-2}	9.47×10^{-4}	15.7
	B	0.960	2.35×10^{-2}	5.54×10^{-4}	16.2
15W2S (16.21)	A	0.907	4.54×10^{-2}	2.13×10^{-3}	35.8
	B	0.829	6.57×10^{-2}	4.15×10^{-3}	28.2

Figure 10 shows the comparison between the measured and simulated vertical profiles. In 15W2S of Figure 10 (b), two simulated curves are not in good agreement with the measured one. The transverse dispersivity in the low velocity region ranges from 2.6×10^{-4} to 4.2×10^{-3} m. In the intermediate velocity region, the values of transverse dispersivity is given in Table 3, and the comparison of vertical profiles between measurement and two simulations is shown in Figure 11. The value of RMSE in the intermediate velocity region is calculated to be less than 35 %. The vertical profiles fitted using the fixed parameters from time moments (Case A) and least squares fitting (Case B) comparatively consist with the observed profiles as shown in Figure 11. The transverse dispersivity in the intermediate region ranges from 1.7×10^{-4} to 1.4×10^{-3} m. Table 4 shows the result of the transverse dispersivity in the high velocity region, and Figure 12 shows the comparison between measured and simulated vertical profiles. The value of RMSE at the borehole of 5W0.5S is much higher than the others and is over 40 %. The estimated vertical profiles at 5W0.5S seem to be out of the measured one, and the values of transverse dispersivities at 5W0.5S is especially high in the high velocity region. The estimated transverse dispersivity at 5W0.5S is removed in all subsequent discussion because it is considered that there is relatively large error in the estimation of transverse dispersivity at 5W0.5S. The transverse dispersivity in the high velocity region ranges from 6.5×10^{-4} to 2.6×10^{-3} m except for the result of 5W0.5S.

There is one peak of concentration for the measured vertical profiles within each velocity region, which are used in previous analyses. During the tracer migration, however, several peaks of concentration in the vertical profile were observed with spreading throughout a few velocity regions. The partial vertical profile restricted by each velocity region was also used in the evaluation of transverse dispersivity. The results of transverse dispersivity calculated from fitting to the partial vertical profile summarized in Table 5. Figure 13 shows the result of fitting to the vertical profile restricted by the low velocity region at the borehole of 5W0.5S at the elapsed time of 4.52 day. The 3-D fitting technique was applied to the observed profile under the elevation of 145.6 m, limited by the low velocity region. The values of transverse dispersivities estimated from fitting to partial profile approximately lie within the range shown in Table 2. The results of partial fitting in the intermediate- and high-velocity region are shown in Figure 14 and Figure 15, respectively. These values of transverse dispersivity based on partial fitting procedure also agree with that estimated in previous calculation in the intermediate- and high-velocity region.

Figure 16 shows the relation between transverse dispersivity and the distance from the injection well. From this figure, there is no influence of the migration scale on the estimated transverse dispersivities in each velocity region.

Figure 17 (a) shows the comparison of transverse dispersivities between Case A (temporal moments) and Case B (least squares fitting). Although a few values of transverse dispersivity in Case A is different from those in Case B, basically most of results in Case A is close to those in Case B. The comparison of the ratio of transverse to longitudinal dispersivity (α_T/α_L) between

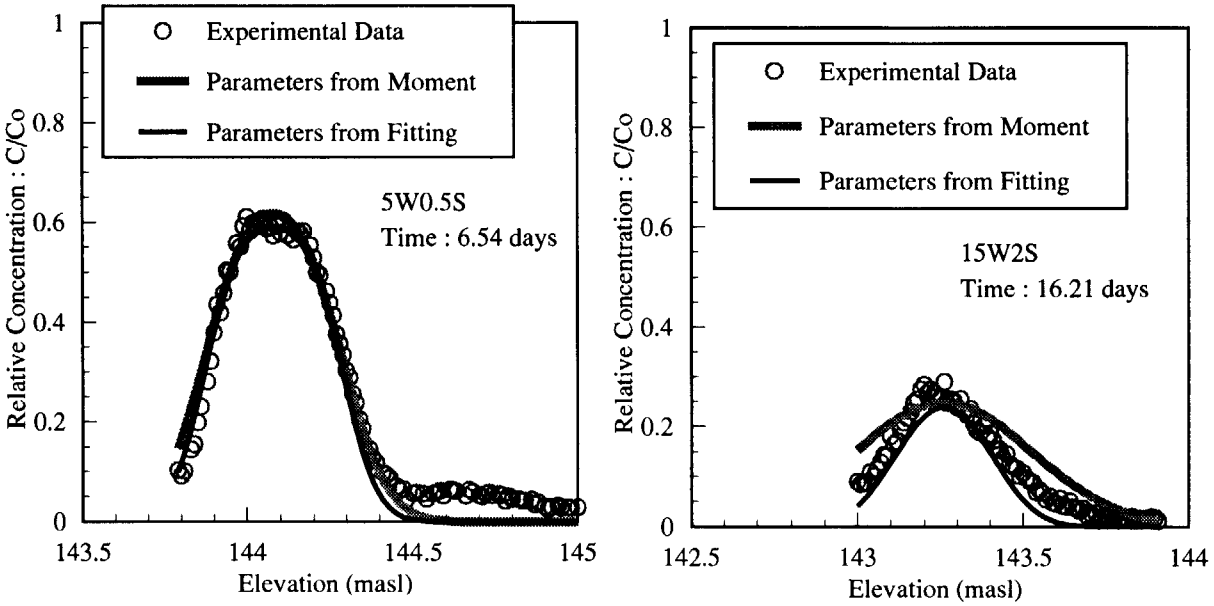

(a) 5W0.5S (Time : 6.54 days)

(b) 15W2S (Time : 16.21 days)

Figure 10 Comparison between measured and simulated vertical profiles determined using input parameters from temporal moments and fitting methods in the low velocity region

Table 3 The result of transverse dispersivity calculated from fitting the three-dimensional solution (4) to measuements in the intermediate velocity region; in Case A using the fixed parameters of velocity and longitudinal dispersivity estimated from temporal moments, in Case B using ones estimated from least squares fitting

Well No. (Time:days)	Case	Velocity : V(m/day)	Longitudinal Dispersivity : α_L (m)	Tnansverse Dispersivity : α_T (m)	RMSE (%)
10W1.5S (8.26)	A	1.17	8.21×10^{-2}	7.69×10^{-4}	30.0
	B	1.23	1.16×10^{-2}	1.37×10^{-3}	28.2
10W1.5S (9.17)	A	1.17	8.21×10^{-2}	4.91×10^{-4}	17.3
	B	1.23	1.16×10^{-2}	7.02×10^{-4}	18.3
15W2S (13.91)	A	1.13	3.59×10^{-2}	6.02×10^{-4}	25.5
	B	1.15	8.80×10^{-3}	6.32×10^{-4}	25.4
20W3S (14.90)	A	1.38	7.32×10^{-2}	2.94×10^{-4}	32.3
	B	1.43	1.20×10^{-2}	1.73×10^{-4}	26.2
25W4S (18.88)	A	1.11	8.51×10^{-2}	2.17×10^{-4}	34.8
	B	1.15	8.78×10^{-3}	1.92×10^{-4}	23.1

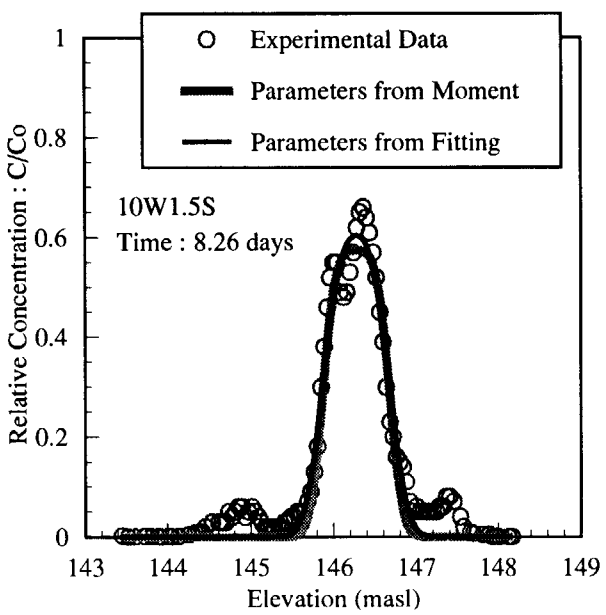

(a) 10W1.5S (Time : 8.26 days)

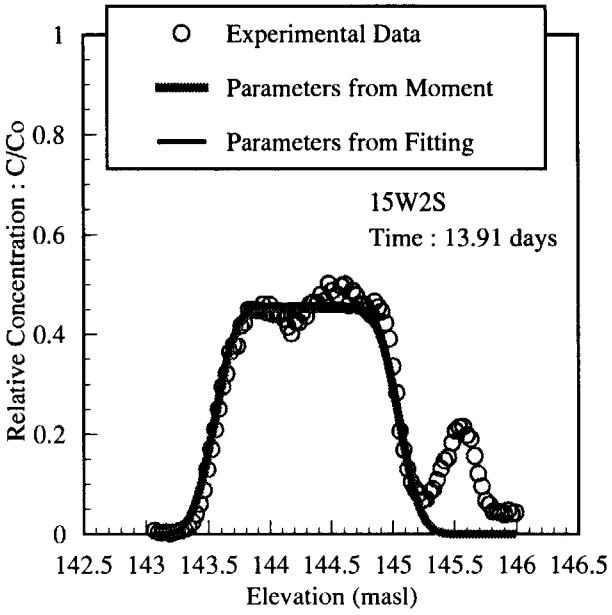

(b) 15W2S (Time : 13.91 days)

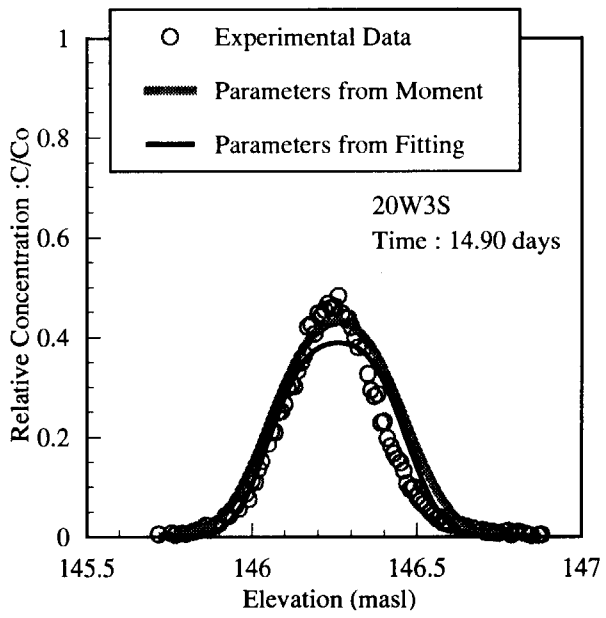

(c) 20W3S (Time : 14.9 days)

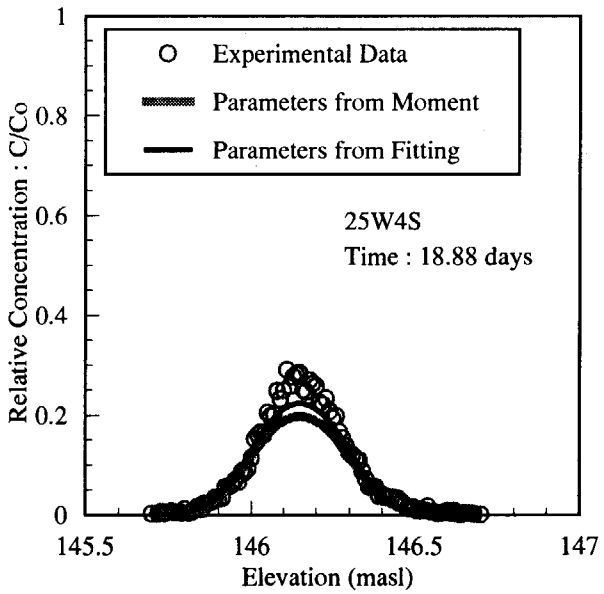

(d) 25W4S (Time : 18.88 days)

Figure 11 Comparison between measured and simulated vertical profiles determined using input parameters from temporal moments and fitting methods in locity region

Table 4 The result of transverse dispersivity calculated from fitting the three-dimensional solution (4) to measuements in the high velocity region; in Case A using the fixed parameters of velocity and longitudinal dispersivity estimated from temporal moments, in Case B using ones estimated from least squares fitting

Well No. (Time:days)	Case	Velocity : V(m/day)	Longitudinal Dispersivity : α_L(m)	Tnansverse Dispersivity : α_T(m)	RMSE (%)
5W0.5S (3.34)	A	1.34	8.73×10^{-2}	6.43×10^{-3}	44.7
	B	1.46	3.49×10^{-2}	1.27×10^{-2}	41.1
10W1.5S (7.23)	A	1.36	1.49×10^{-1}	2.60×10^{-3}	24.2
	B	1.45	2.15×10^{-2}	2.61×10^{-3}	24.2
15W2S (10.85)	A	1.33	1.87×10^{-1}	6.50×10^{-4}	12.4
	B	1.44	1.57×10^{-2}	1.28×10^{-3}	33.3

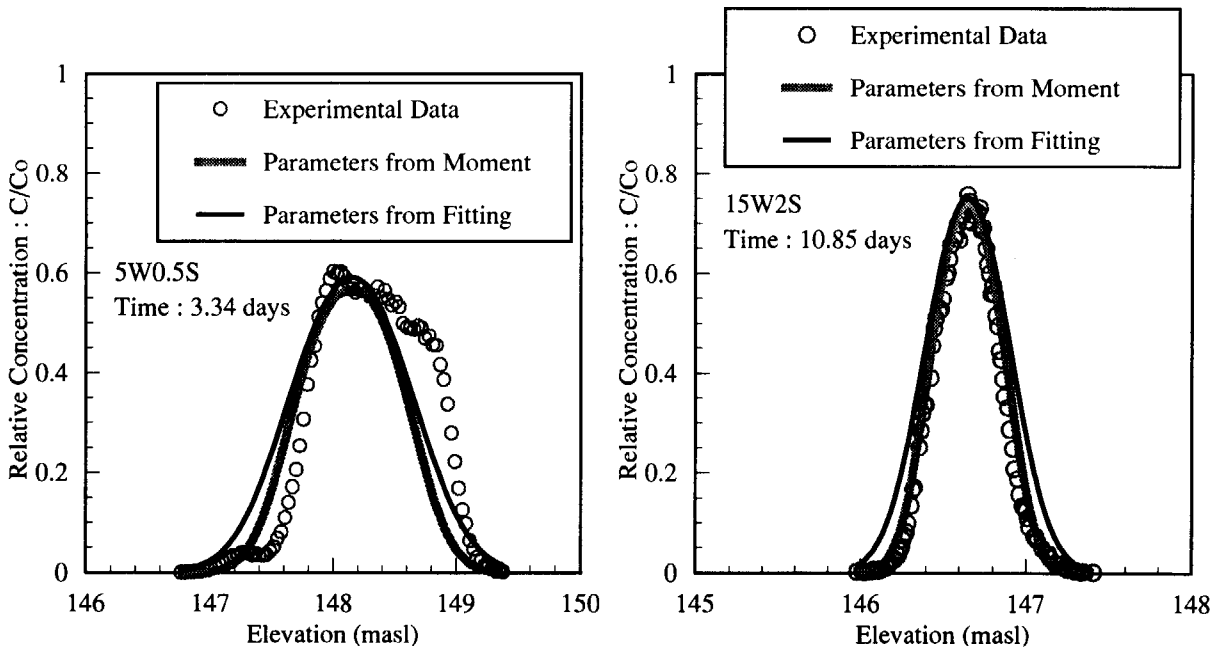

(a) 5W0.5S (Time : 3.34 days) (b) 15W2S (Time : 10.85 days)

Figure 12 Comparison between measured and simulated vertical profiles determined using input parameters from Integrating (temporal moments) and fitting (least squares fitting) methods in the high velocity region

Table 5 The result of transverse dispersivity calculated from applying the 3-D least squares fitting to vertical profile restricted by each velocity region; in Case A using the fixed parameters of velocity and longitudinal dispersivity estimated from temporal moments, in Case B using ones estimated from least squares fitting

Well No. (Time:days)	Type of Velocity Region	Case	Velocity : V(m/day)	Longitudinal Dispersivity : α_L(m)	Tnansverse Dispersivity : α_T(m)	RMSE (%)
5W0.5S (4.52)	Low	A	0.932	5.31×10^{-2}	1.75×10^{-3}	7.4
		B	0.960	2.35×10^{-2}	4.70×10^{-3}	8.3
35W6S (29.91)	Intermediate	A	1.09	2.13×10^{-1}	1.81×10^{-4}	17.0
		B	1.16	9.40×10^{-3}	5.71×10^{-4}	18.3
40W7S (33.90)	Intermediate	A	1.14	8.31×10^{-2}	8.54×10^{-4}	10.7
		B	1.18	1.08×10^{-2}	8.27×10^{-4}	10.6
5W0.5S (4.52)	High	A	1.34	8.73×10^{-2}	3.17×10^{-3}	33.1
		B	1.46	3.49×10^{-2}	1.76×10^{-3}	34.9
15W2S (13.36)	High	A	1.33	1.87×10^{-1}	1.52×10^{-3}	30.5
		B	1.44	1.57×10^{-2}	1.41×10^{-3}	30.3

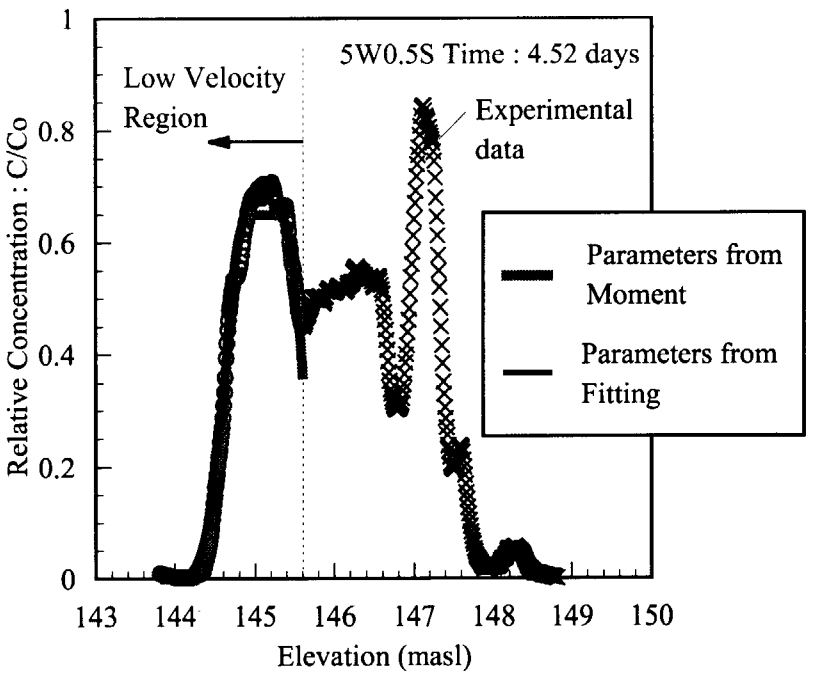

Figure 13 Fitting to the vertical profile restricted by the low velocity region at the borehole of 5W0.5S (Time : 4.52 days)

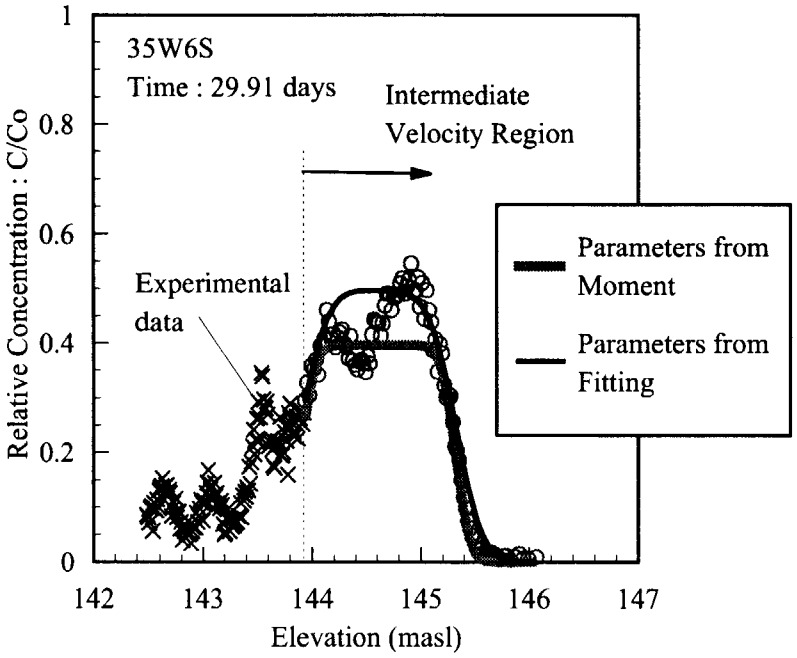

(a) 35W6S (Time : 29.91 days)

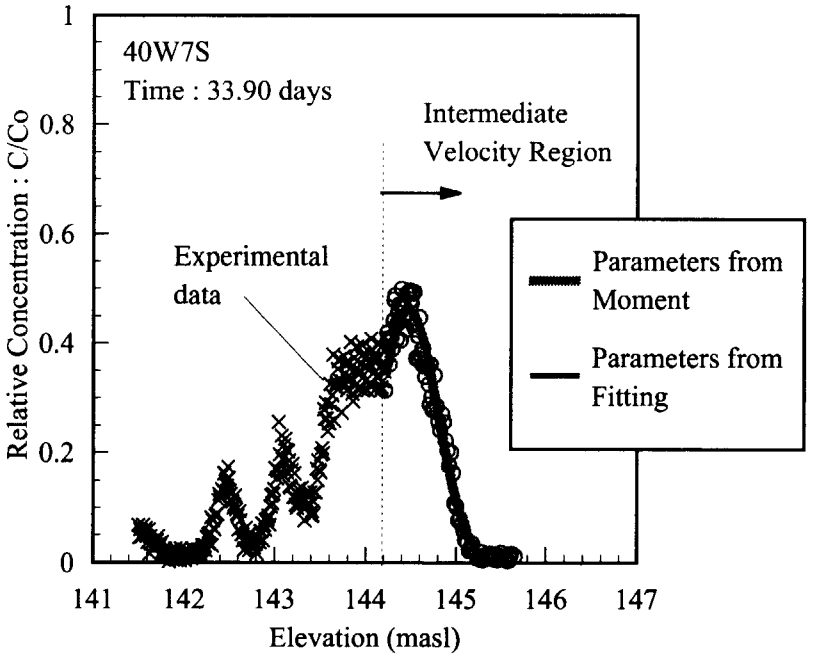

(b) 40W7S (Time : 33.90days)

Figure 14 Fitting to the vertical profile restricted by the intermediate velocity region at the borehole of 35W6S (Time : 29.91 days) and 40W7S (Time : 33.90days)

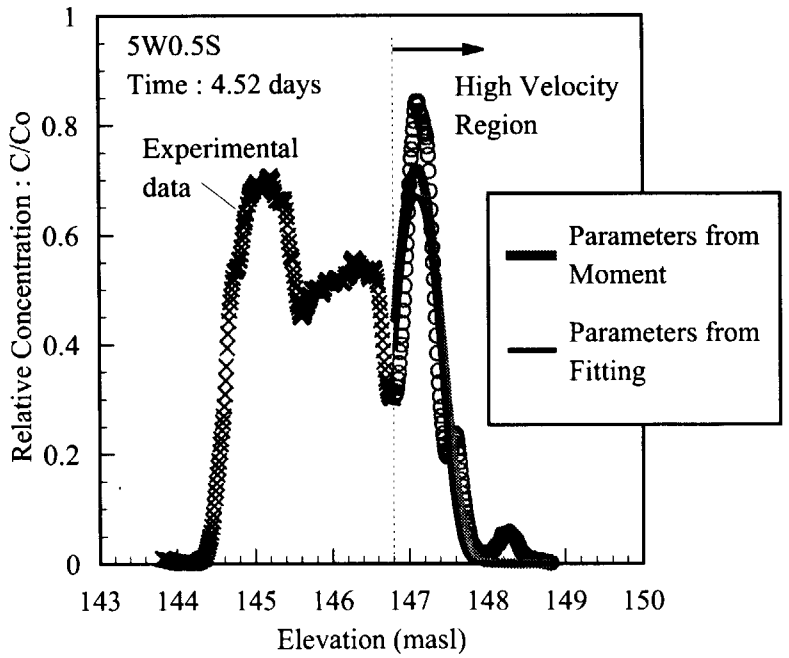

(a) 5W0.5S (Time : 4.52 days)

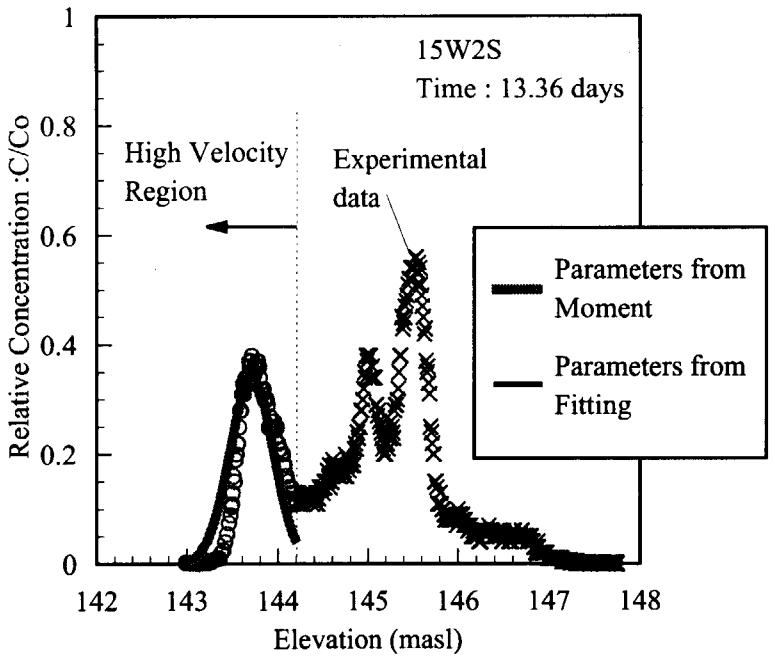

(b) 15W2S (Time : 13.36 days)

Figure 15 Fitting to the vertical profile restricted by the high velocity region at the borehole of 5W0.5S (Time : 4.52 days) and 15W2S (Time : 13.36 days)

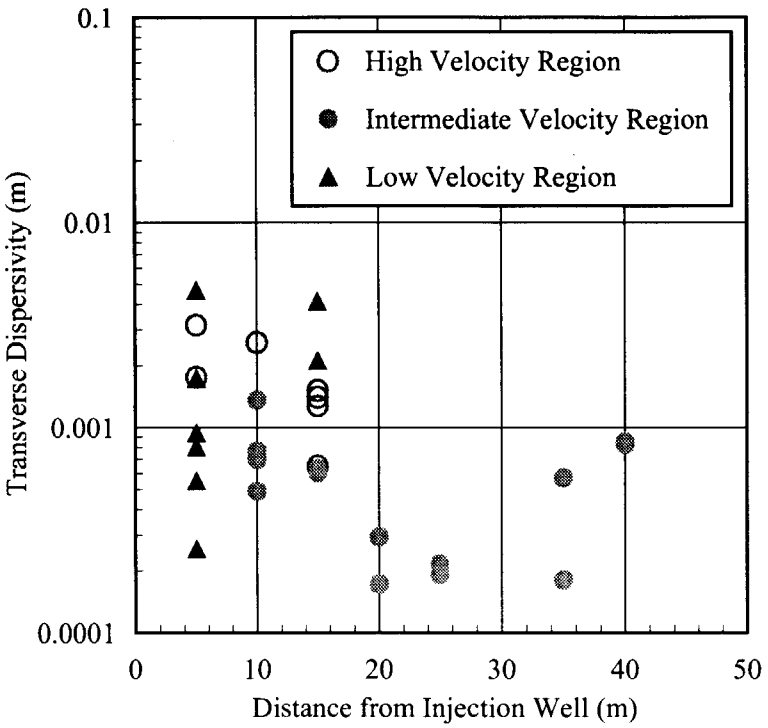

Figure 16 Influence of the migration scale on the estimated transverse disversivitis in each velocity region

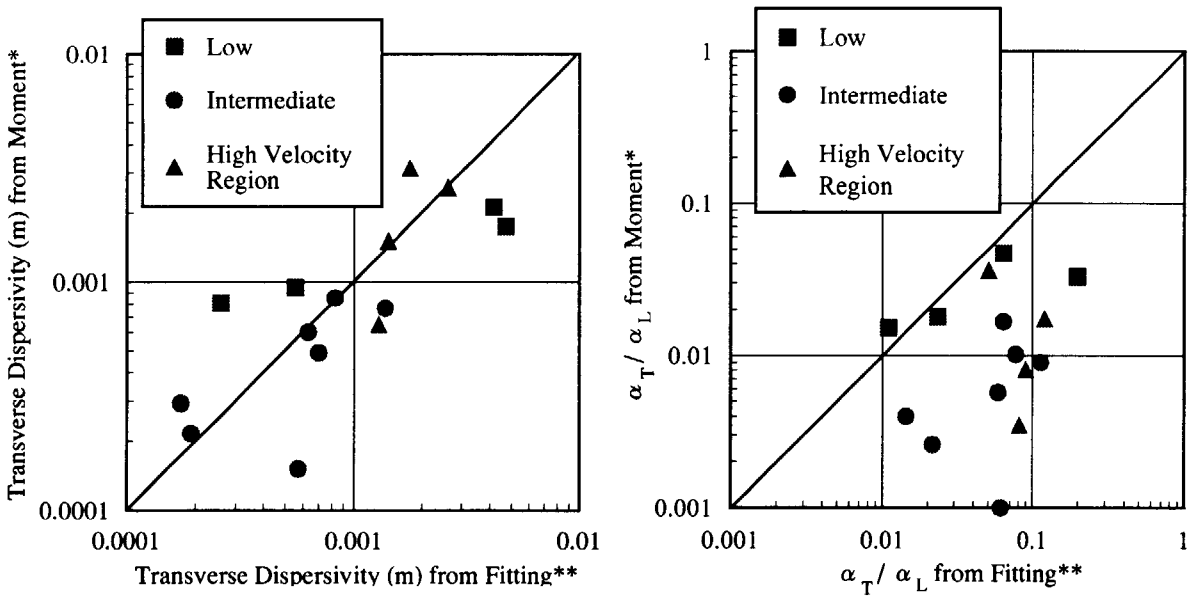

(a) Transverse Dispersivity (b) Transverse / Longitudinal Dispersivity

Figure 17 Comparison between temporal moments and least square fitting in each velocity region

Case A and Case B is given in Figure 17 (b). The values of α_T/α_L estimated in Case A tend to be lower than those estimated in Case B. The under-estimation of this ratio in Case A is caused by the trend of higher longitudinal dispersivity estimated using temporal moments method.

Figure 18 shows the variance of transverse dispersivity and α_T/α_L estimated from the three-dimensional least squares fitting method in each velocity region. The average values of these estimated parameters are shown in Table 6. The transverse dispersivity in the intermediate-velocity region is lower than one in the low- and high-velocity region. The mean transverse dispersivities in the high velocity region is about 5 factor of magnitude higher than that in the intermediate velocity region. The value of α_T/α_L for the intermediate velocity region tends to be lower than the others on account of low transverse dispersivity, however, the tendency is not

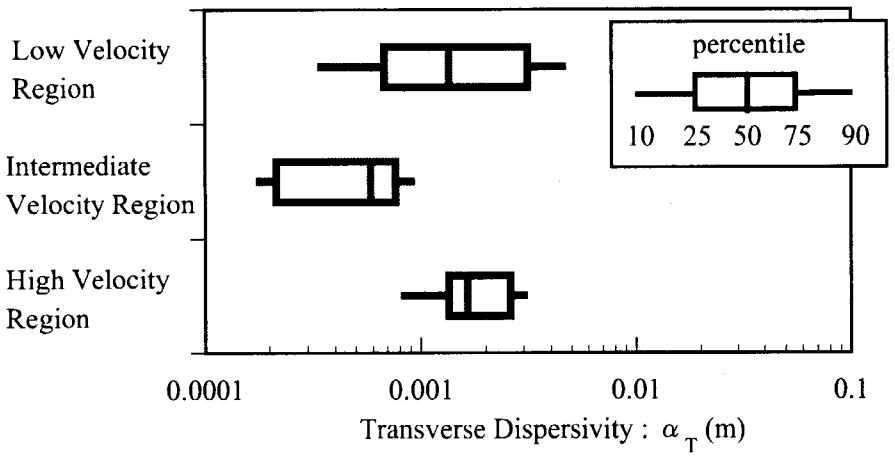

(a) Transverse Dispersivity

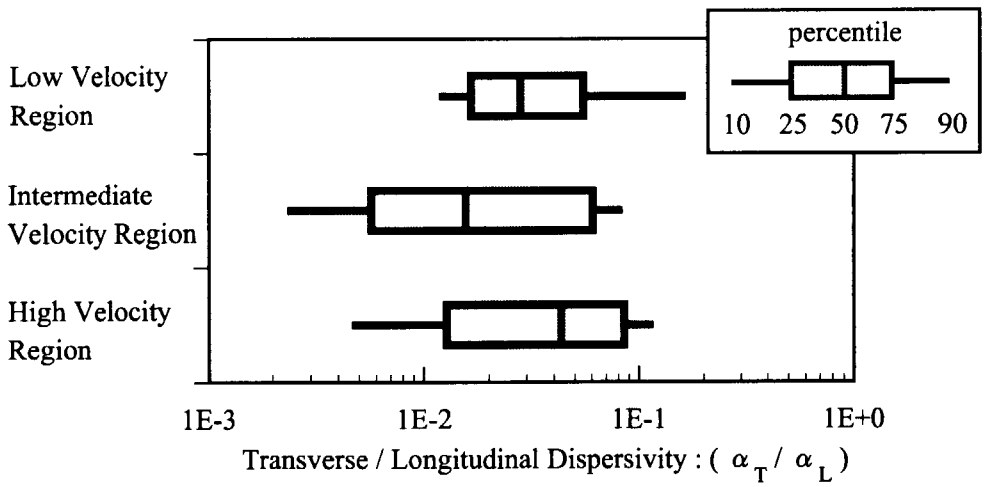

(b) Ratio of Tansverse to Longitudinal dispersivity

Figure 18 Variance of the estimated transverse dispersivity and the ratio of transverse to longitudinal dispersivity in the low-, intermediate- and high-velocity region

Table 6 Average values of the estimated transverse dispersivity and the ratio of transverse to longitudinal dispersivity

Estimeted Parameters	High Velocity Region	Intermediate Velocity Region	Low Velocity Region
Mean Transverse Dispersivity : m	2.87×10^{-3}	5.95×10^{-4}	1.38×10^{-3}
Mean α_T/α_L	0.072	0.043	0.051

so remarkable. The value of α_T/α_L approximately ranges from 0.002 to 0.2. Mean values of α_T/α_L in the high-, intermediate- and low-velocity region are 0.072, 0.043 and 0.051, respectively. Calibration of this ratio in the simulation of both chloride and tritium concentration in the Lake 233 basin including the Twin Lake tracer test site has been carried out by Takeda, Klukas et al. (1998)[10], and yielded the ratio of transverse to longitudinal dispersivity of 0.05. This calibrated ratio lies within the mean values of α_T/α_L estimated in this work.

6. Conclusion

The concentration data of ^{131}I from the 40 m tracer test were analyzed to evaluate the mass transport parameters in the Twin Lake test site. The velocity and longitudinal dispersivity were estimated from applying two different methods to the observed breakthrough curves. One method is the one-dimensional least squares fitting, and another is the temporal moments method. Based on the estimated values of velocities and longitudinal dispersivities, the transverse dispersivities were determined from fitting the three-dimensional dispersive-advective solution to the measured vertical profiles. The conclusion of this work is summarized as follow.

There is little difference on the estimated velocity between temporal moments and least squares fitting. The mean velocities in the high-, intermediate- and low-velocity region are 1.28, 1.16, 0.997 m/day, respectively. The result of the estimated velocity agrees with the classification of velocity zone determined by Killey and Moltyaner (1988)[5].

In the low velocity region, the values of longitudinal dispersivity estimated from temporal moments are comparatively close to that from the least squares fitting, however, all values of longitudinal dispersivity from temporal moment are higher than that from fitting procedure in the intermediate- and high-velocity region. It is considered that discrepancy of longitudinal dispersivity between temporal moments and fitting method is caused by the effect of trailing tail observed in the breakthrough curves in the intermediate- and high-velocity region. It is suggested that the longitudinal dispersivity calculated using both time moments and least squares fitting methods depends on the trailing tail in measured breakthrough curve.

The mean longitudinal dispersivity in the high-, intermediate- and low-velocity region are 8.8×10^{-2}, 5.3×10^{-2} and 6.2×10^{-2} m, respectively. The estimated longitudinal dispersivity is hardly influenced by the heterogeneity in three kinds of velocity region.

Although the trend of increasing longitudinal dispersivity as a function of measurement scale can be slightly observed in the low velocity region, basically, there is no effect of the travel distance on both the longitudinal and transverse dispersivities in 40 m tracer scale.

The measured vertical profiles characterized by several peaks of concentration are particularly restricted by three kinds of velocity regions and used in the estimation of transverse dispersivity besides the profiles with one peak. The values of transverse dispersivities calculated from fitting to partial profile are consistent with the results obtained from fitting to the vertical profile characterized by one peak of concentration.

The mean transverse dispersivity in the high-, intermediate- and low-velocity region are 2.9×10^{-3}, 6.0×10^{-4} and 1.4×10^{-3} m, respectively. The transverse dispersivity in the intermediate-velocity region tends to be lower than one in the low- and high-velocity region. Mean values of the ratio of the transverse to longitudinal dispersivity (α_T / α_L) in the high-, intermediate- and low-velocity region are 0.072, 0.043 and 0.051, respectively. The ratio of 0.05, calibrated using 3-D model for the basin scale at the Lake 233 site [Takeda, Klukas et al. (1998)[10]], lies within the mean values of α_T / α_L estimated in this work.

Acknowledgment

We would like to thank Dr. M. H. Klukas for valuable discussion on the interpretation of the estimated parameters, and Dr. C. A. Wills and L. Yamazaki for valuable discussion and support of borehole data base at Twin Lake tracer tests.

References

(1) Moltyaner, G. L. and Paniconi, C. : Migration of Radionuclides in Porus Media, Analysis of experimental data, AECL-8254 (1984).
(2) Moltyaner, G. L. and Killy, R. W. D. : Twin Lake Tests : Longitudinal Dispersion, Water Resources Research, Vol. 24, No. 10, 1613-1627 (1988a).
(3) Devary, J. L. and Simmons, C. L. : Groundwater Model Parameter Estimation Using a Stochastic-Convective Approach, EPRI CS-3629 (1984).
(4) Moltyaner, G. L. and Wills, C. A. : Method of Moments Analysis of the Twin Lake Tracer Test Data, AECL-9521 (1987).
(5) Killy, R. W. D. and Moltyaner, G. L. : Twin Lake Tests: Setting, Methodology, and Hydraulic Conductivity Distribution, Water Resources Research, Vol. 24, No. 10, p1585-1612 (1988).
(6) Bear, J. : Dynamic of Fluids in Porous Media, Elservier Science, New York, (1972).
(7) Moltyaner, G. L. and Killy, R. W. D. : Twin Lake Tests : Transverse Dispersion, Water Resources Research, Vol. 24, No. 10, 1628-1637 (1988b).
(8) Van der Laan, E. : Statistical and graphical methods for evaluating solute transport models : Overview and application, J. Contam. Hydrol., Vol. 7, 51-73 (1991).
(9) Loague, K. and Green, R. E. : Statistical and graphical methods for evaluating solute transport models : Overview and application, J. Contam. Hydrol., Vol. 7, 51-73 (1991).
(10) Takeda, S., Klukas, M. H., Moltyaner, G. L., Kotzer, T. andYamazaki, L. : Advection Dispersion Modelling of Tritium and Chloride Migration in a Shallow Sandy Aquifer at the Chalk River Laboratory Site, Submitted to Research Coordination Meeting on Use of Isotopes for Analyses of Flow and Transport Dynamics, in Virginia (1998).

国際単位系（SI）と換算表

表1　SI基本単位および補助単位

量	名称	記号
長さ	メートル	m
質量	キログラム	kg
時間	秒	s
電流	アンペア	A
熱力学温度	ケルビン	K
物質量	モル	mol
光度	カンデラ	cd
平面角	ラジアン	rad
立体角	ステラジアン	sr

表2　SIと併用される単位

名称	記号
分，時，日	min, h, d
度，分，秒	°, ′, ″
リットル	l, L
トン	t
電子ボルト	eV
原子質量単位	u

1 eV=1.60218×10^{-19}J

1 u=1.66054×10^{-27}kg

表3　固有の名称をもつSI組立単位

量	名称	記号	他のSI単位による表現
周波数	ヘルツ	Hz	s^{-1}
力	ニュートン	N	$m\cdot kg/s^2$
圧力，応力	パスカル	Pa	N/m^2
エネルギー,仕事,熱量	ジュール	J	N·m
工率，放射束	ワット	W	J/s
電気量，電荷	クーロン	C	A·s
電位，電圧，起電力	ボルト	V	W/A
静電容量	ファラド	F	C/V
電気抵抗	オーム	Ω	V/A
コンダクタンス	ジーメンス	S	A/V
磁束	ウェーバ	Wb	V·s
磁束密度	テスラ	T	Wb/m^2
インダクタンス	ヘンリー	H	Wb/A
セルシウス温度	セルシウス度	℃	
光束	ルーメン	lm	cd·sr
照度	ルクス	lx	lm/m^2
放射能	ベクレル	Bq	s^{-1}
吸収線量	グレイ	Gy	J/kg
線量等量	シーベルト	Sv	J/kg

表4　SIと共に暫定的に維持される単位

名称	記号
オングストローム	Å
バーン	b
バール	bar
ガル	Gal
キュリー	Ci
レントゲン	R
ラド	rad
レム	rem

1 Å=0.1nm=10^{-10}m

1 b=100fm^2=10^{-28}m^2

1 bar=0.1MPa=10^{5}Pa

1 Gal=1cm/s^2=10^{-2}m/s^2

1 Ci=3.7×10^{10}Bq

1 R=2.58×10^{-4}C/kg

1 rad=1cGy=10^{-2}Gy

1 rem=1cSv=10^{-2}Sv

表5　SI接頭語

倍数	接頭語	記号
10^{18}	エクサ	E
10^{15}	ペタ	P
10^{12}	テラ	T
10^{9}	ギガ	G
10^{6}	メガ	M
10^{3}	キロ	k
10^{2}	ヘクト	h
10^{1}	デカ	da
10^{-1}	デシ	d
10^{-2}	センチ	c
10^{-3}	ミリ	m
10^{-6}	マイクロ	μ
10^{-9}	ナノ	n
10^{-12}	ピコ	p
10^{-15}	フェムト	f
10^{-18}	アト	a

(注)

1．表1－5は「国際単位系」第5版，国際度量衡局1985年刊行による。ただし,1 eVおよび1 uの値はCODATAの1986年推奨値によった。

2．表4には海里，ノット，アール，ヘクタールも含まれているが日常の単位なのでここでは省略した。

3．barは，JISでは流体の圧力を表わす場合に限り表2のカテゴリーに分類されている。

4．EC閣僚理事会指令ではbar，barnおよび「血圧の単位」mmHgを表2のカテゴリーに入れている。

換算表

力	N(=10^{5}dyn)	kgf	lbf
	1	0.101972	0.224809
	9.80665	1	2.20462
	4.44822	0.453592	1

粘度　1 Pa·s(N·s/m^2)=10 P(ポアズ)(g/(cm·s))

動粘度　1m^2/s=10^{4}St(ストークス)(cm^2/s)

圧力	MPa(=10bar)	kgf/cm^2	atm	mmHg(Torr)	lbf/in^2(psi)
	1	10.1972	9.86923	7.50062×10^3	145.038
	0.0980665	1	0.967841	735.559	14.2233
	0.101325	1.03323	1	760	14.6959
	1.33322×10^{-4}	1.35951×10^{-3}	1.31579×10^{-3}	1	1.93368×10^{-2}
	6.89476×10^{-3}	7.03070×10^{-2}	6.80460×10^{-2}	51.7149	1

エネルギー・仕事・熱量	J(=10^7 erg)	kgf·m	kW·h	cal(計量法)	Btu	ft·lbf	eV
	1	0.101972	2.77778×10^{-7}	0.238889	9.47813×10^{-4}	0.737562	6.24150×10^{18}
	9.80665	1	2.72407×10^{-6}	2.34270	9.29487×10^{-3}	7.23301	6.12082×10^{19}
	3.6×10^6	3.67098×10^5	1	8.59999×10^5	3412.13	2.65522×10^6	2.24694×10^{25}
	4.18605	0.426858	1.16279×10^{-6}	1	3.96759×10^{-3}	3.08747	2.61272×10^{19}
	1055.06	107.586	2.93072×10^{-4}	252.042	1	778.172	6.58515×10^{21}
	1.35582	0.138255	3.76616×10^{-7}	0.323890	1.28506×10^{-3}	1	8.46233×10^{18}
	1.60218×10^{-19}	1.63377×10^{-20}	4.45050×10^{-26}	3.82743×10^{-20}	1.51857×10^{-22}	1.18171×10^{-19}	1

1 cal= 4.18605J（計量法）

= 4.184J（熱化学）

= 4.1855J（15℃）

= 4.1868J（国際蒸気表）

仕事率　1 PS(仏馬力)

= 75 kgf·m/s

= 735.499W

放射能	Bq	Ci
	1	2.70270×10^{-11}
	3.7×10^{10}	1

吸収線量	Gy	rad
	1	100
	0.01	1

照射線量	C/kg	R
	1	3876
	2.58×10^{-4}	1

線量当量	Sv	rem
	1	100
	0.01	1

(86年12月26日現在)

ESTIMATION OF LONGITUDINAL AND TRANSVERSE DISPERSIVITIES IN THE TWIN LAKE NATURAL GRADIENT TRACER TESTS